Modeling spatial effects in multi-longitudinal-mode semiconductor lasers

C. Serrat[1] and C. Masoller[1,2]
[1]*Departament de Física i Enginyeria Nuclear, Universitat Politècnica de Catalunya, Colom 11, E-08222 Terrassa, Spain*
[2]*Instituto de Física, Facultad de Ciencias, Universidad de la República, Iguá 4225, Montevideo 11400, Uruguay*
(Received 23 November 2005; published 25 April 2006)

The multi-longitudinal-mode dynamics of a semiconductor laser is studied theoretically, based on traveling-wave equations for the slowly varying amplitudes of the counterpropagating optical fields in the laser cavity, coupled to an equation for the carrier population dynamics. The model considers key ingredients describing the semiconductor medium, such as the spatial variations of the carriers and optical fields in the longitudinal direction, a parabolic frequency-dependent gain and phase-amplitude coupling, and does not assume *a priori* a fixed number of active longitudinal modes. We find deterministic out-of-phase modal oscillations which leave the sum of total modal intensities nearly constant. These oscillations become faster as the injection current increases, in good agreement with recent experimental observations. In our model the origin of modal oscillations is spatial hole burning in the envelope of the carrier grating, which is due to the interaction of different longitudinal modes. We also observe switching and hopping of the lasing modes in accordance with the experiments.

DOI: 10.1103/PhysRevA.73.043812 PACS number(s): 42.60.Mi, 05.45.−a

I. INTRODUCTION

Semiconductor lasers are widely used as coherent light sources in optical communication systems. Multi-longitudinal-mode operation is detrimental for the use of semiconductor lasers in applications that require a narrow spectral linewidth, but it is needed for multiplexed optical communications, and is also desirable for applications that require large output power. Two sources of power fluctuations are mode partition (which refers to a leakage of power into side modes and results in a fast modulation of the total output), and mode hopping (which refers to sudden drops of the main mode power accompanied by the sudden excitation of a side mode). Mode partition and mode hopping in *bulk* semiconductor lasers have been extensively studied and successfully explained in terms of noise-driven phenomena originating from spontaneous emission noise and the coupling among modes; however, a recent study of *quantum-well* semiconductor lasers demonstrated the existence of deterministic nonlinear dynamics in the multimode operation of free-running lasers [1]. This dynamics is characterized by (i) periodic oscillations (in the megahertz range) of the power of each longitudinal mode; (ii) a compensation on the total power (which is nearly constant in time), and (iii) a switching sequence related to the optical frequencies of the modes (the switching goes from the bluest to the reddest mode). A detailed comparison of the periodic switching occurring in quantum-well lasers with the mode hopping occurring in bulk lasers was carried out in [2], where the differences between the multimode behavior of bulk and quantum-well lasers were interpreted as due to the interaction among the optical waves inside the laser cavity. In [1] the experimental observations were explained within the framework of two models that include the susceptibility of quantum-well active media and four-wave-mixing processes for the longitudinal modes. Similar switching phenomena has also been observed in a rate-equation model that includes self- and cross-saturation coefficients for the modal gains [3,4]. These two explanations for the periodic switching dynamics are complementary since the four-wave-mixing mechanism taken into account in [1] can be traced down to asymmetric cross-saturation coefficients, which can be due to either a large linewidth enhancement factor or, more realistically in quantum-well lasers, a large differential material gain. The fact that the switching dynamics of quantum-well lasers is almost insensitive to current noise or current modulation [2] but highly sensitive to weak optical feedback [5] reinforces four-wave mixing as the driving mechanism of the switching behavior.

In this paper we explore a complementary mechanism leading to mode switching and mode hopping, based on spatial hole-burning effects. Our study is motivated by the results of Homar *et al.* [6,7], who studied the dynamics of a Fabry-Pérot semiconductor laser within the framework of a traveling-wave model. When the semiconductor medium was described as a two-level medium [6], complex multimode dynamics was observed, but mode hopping was not found. However, with a more realistic description of the semiconductor medium (including asymmetric frequency-dependent gain and refractive index), mode hopping can occur (see Fig. 4 of [7]), and was interpreted as due to changes in the modal gain curve induced by spatial hole burning. The aim of the present work is to further analyze the multimode dynamics of semiconductor lasers, based on a traveling-wave model similar to the one employed by Homar *et al.* [6,7], which avoids *a priori* assumptions on the number of active longitudinal modes, considers spatial variations in the longitudinal direction, and incorporates key ingredients describing the semiconductor medium (frequency-dependent parabolic gain and phase-amplitude coupling).

The model studied in this paper consist of two equations for the counterpropagating optical fields in the laser cavity coupled to an equation for the carrier population dynamics, and has been employed to describe multimode lasers with optical injection [8], with optical feedback [9–11], and the synchronization of multimode lasers, [12]. However, in all

these studies, the approximations involved in the model and, in particular, the relation to other multimode models have not been explicitly addressed. Here we present a derivation of the model that shows its equivalence with models where only the "slow" spatial grating in the carrier density (due to interference effects of the longitudinal modes) is taken into account, while the "fast" spatial grating (at half the optical wavelength, due to the counterpropagating optical fields) is neglected [1,14]. Physically, this approximation is valid because typical carrier diffusion rates for conduction-band electrons imply that diffusion can wash out a grating with a spacing of half a wavelength on a fast time scale, but is not fast enough to wash out a grating with a long characteristic length (of the order of the cavity length). We show that spatial hole-burning effects on the envelope of the carrier density are enough to induce anticorrelated oscillations of the modal intensities. No stochastic forces are required to induce (or sustain) such oscillations.

The paper is organized as follows. In Sec. II we present a derivation of the model and identify the relevant approximations. In Sec. III we discuss monochromatic approximated solutions that are associated with the longitudinal modes of the active cavity. In Sec. IV we present results of numerical simulations, which show that for typical parameters corresponding to multimode operation, the modal intensities exhibit anticorrelated deterministic oscillations which result in a nearly perfect compensation of the sum of modal intensities. These oscillations become faster as the injection current increases, in good agreement with experimental observations [1]. We analyze mode-switching and -hopping effects which appear as the injection current is increased from the lasing threshold, and also study the effects of carrier diffusion. Section V presents a summary and the conclusions.

II. MODEL

To present a derivation of the model, we begin with the Maxwell second-order differential equation for a linearly polarized classical optical field $\mathcal{E}$,

$$\left(\frac{\partial^2}{\partial z^2}-\frac{\eta^2}{c^2}\frac{\partial^2}{\partial t^2}\right)\mathcal{E}(z,t)=\frac{1}{\epsilon_0 c^2}\frac{\partial^2}{\partial t^2}\mathcal{P}(z,t), \tag{1}$$

where ϵ_0 is the vacuum permittivity, c is the speed of light in vacuum, η is the background refractive index, and $\mathcal{P}$ represents the polarization induced by the active population inversion. The omplex field and the material variables are assumed to depend only on the longitudinal variable z, the dependence on the transverse variables being neglected. The optical field and the polarization can be written as

$$\mathcal{E}(z,t)=E(z,t)e^{-i\omega_0 t}+\text{c.c.}, \tag{2}$$

$$\mathcal{P}(z,t)=P(z,t)e^{-i\omega_0 t}+\text{c.c.}, \tag{3}$$

where $E(z,t)=E^+(z,t)e^{ik_0 z}+E^-(z,t)e^{-ik_0 z}$, with $E^+(z,t)$ and $E^-(z,t)$ being the slowly varying (in time and space) complex amplitudes of the fields circulating forward and backward in the Fabry-Pérot laser cavity, ω_0 an arbitrary reference frequency, and k_0 is the corresponding propagation constant ($k_0=\eta\omega_0/c$). $P(z,t)$ is the slowly varying (in time) complex amplitude of the polarization which keeps the fast z dependence.

The slowly-varying-envelope approximation gives the following equations for $E^+(z,t)$ and $E^-(z,t)$ [6]:

$$\frac{\eta}{c}\frac{\partial E^+}{\partial t}+\frac{\partial E^+}{\partial z}=\frac{i\omega_0}{2\epsilon_0 c\eta}\langle P(z,t)e^{-ik_0 z}\rangle, \tag{4}$$

$$\frac{\eta}{c}\frac{\partial E^-}{\partial t}-\frac{\partial E^-}{\partial z}=\frac{i\omega_0}{2\epsilon_0 c\eta}\langle P(z,t)e^{ik_0 z}\rangle, \tag{5}$$

where $\langle\cdots\rangle$ means a spatial average over many wavelengths. Assuming that the polarization can be adiabatically eliminated and that $P(z,t)=\epsilon_0\chi E(z,t)$, where χ is the complex susceptibility, we obtain

$$\frac{\eta}{c}\frac{\partial E^+}{\partial t}+\frac{\partial E^+}{\partial z}=\frac{i\omega_0}{2c\eta}\langle\chi E^+\rangle, \tag{6}$$

$$\frac{\eta}{c}\frac{\partial E^-}{\partial t}-\frac{\partial E^-}{\partial z}=\frac{i\omega_0}{2c\eta}\langle\chi E^-\rangle, \tag{7}$$

where we have considered that the quantities $\chi E^+e^{2ik_0 z}$ and $\chi E^-e^{-2ik_0 z}$ average to zero over many wavelengths.

The averages $\langle\chi E^\pm\rangle$ describe the physics of the semiconductor material and allow us to incorporate the main results of the microscopic theories (frequency-dependent gain and phase-amplitude coupling) in a phenomenological way. Assuming that the reference frequency ω_0 is close to the gain peak, a parabolic approximation of the susceptibility in the frequency domain is

$$\chi(\omega,\mathcal{N})=\eta^2\frac{a}{k_0}\left[-\alpha\mathcal{N}-i(\mathcal{N}-\mathcal{N}_0)\left(1-\frac{\omega^2}{\Delta\omega_g^2}\right)\right], \tag{8}$$

where a is the linear gain coefficient, α is the linewidth enhancement factor, $\Delta\omega_g=2\pi\Delta\nu_g$, with $\Delta\nu_g$ being the gain bandwidth (of the order of terahertz), $\mathcal{N}$ is the carrier density, and $\mathcal{N}_0$ is the carrier density at transparency. If we assume that the background refractive index η is frequency independent (i.e., neglecting the dispersive nature of the passive cavity) we can take the inverse Fourier transform using the dispersion relation $\omega=ck/\eta\rightarrow c/\eta(-i\partial/\partial z)$ and obtain

$$\frac{\eta}{c}\frac{\partial E^\pm}{\partial t}\pm\frac{\partial E^\pm}{\partial z}=\frac{a}{2}\left[-i\alpha\mathcal{N}+(\mathcal{N}-\mathcal{N}_0)\left(1+G_d L^2\frac{\partial^2}{\partial z^2}\right)\right]E^\pm-\alpha_i E^\pm, \tag{9}$$

where $G_d=(c/2\pi L\eta\Delta\nu_g)^2$, and we have also included the nonradiative cavity losses α_i.

The equation for the carrier density is

$$\frac{\partial\mathcal{N}}{\partial t}=\mathcal{J}-\gamma\mathcal{N}+\frac{4\epsilon_0}{\hbar}\,\text{Im}(\chi)\left|E^+e^{ik_0 z}+E^-e^{-ik_0 z}\right|^2+D\frac{\partial^2\mathcal{N}(z,t)}{\partial z^2}, \tag{10}$$

where $\mathcal{J}=J/(edwL)$ is the injection current density (J is the injection current, e is the electron charge, d is the quantum-well thickness, w is the current stripe width, and L is the

length of the laser cavity), $\gamma_\parallel$ is the carrier decay rate, and D is the diffusion coefficient.

We assume that the carrier density can be expressed as a "fast" periodic function (a grating with a spacing of half a wavelength that can be written as a Fourier expansion) with a slowly varying envelope $N(z,t)$ [6]:

$$\mathcal{N}(z,t) = N(z,t)\left(1 + \sum N_p(t)(e^{2ipk_0z} + e^{-2ipk_0z})\right). \quad (11)$$

In the following we assume that terms proportional to $e^{\pm 2ipk_0z}$ do not contribute to the dynamical evolution of the slowly varying quantities $E^{\pm}(z,t)$ and $N(z,t)$, because they average to zero over a few wavelengths. This simplification leads to the equations

$$\frac{\eta}{c}\frac{\partial E^{\pm}}{\partial t} \pm \frac{\partial E^{\pm}}{\partial z} = \frac{a}{2}\left[-i\alpha N + (N-\mathcal{N}_0)\left(1 + G_d L^2 \frac{\partial^2}{\partial z^2}\right)\right]E^{\pm} - \alpha_i E^{\pm}, \quad (12)$$

$$\frac{\partial N}{\partial t} = \mathcal{J} - \gamma N - \frac{4\epsilon_0}{\hbar}\frac{\eta^2 a}{k_0}(N-\mathcal{N}_0)(|E^+|^2 + |E^-|^2) + D\frac{\partial^2 N}{\partial z^2}. \quad (13)$$

Note that in Eq. (13) the term $(1+G_d\partial^2/\partial z^2)$ has been neglected in order to be consistent with the approximation that neglects terms proportional to $e^{\pm 2ipk_0z}$. As discussed in the introduction, the fast grating is due to the holes burned by the counterpropagating optical fields, while the slow envelope (with a characteristic length that can be of the order of the cavity length; see, e.g., Figs. 1–3 of [13]) is due to the interaction of the different longitudinal modes. As mentioned above, while carrier diffusion in semiconductor media is typically fast enough to wash out the fast grating, it is not fast enough to wash out the slow grating, which has to be taken into account. We will show in the next section that the multimode dynamics predicted by our model agrees qualitatively well with experimental observations in bulk semiconductor lasers [2].

The final step for the derivation of the model as it is presented in Refs. [8–12] is to rescale the variables as

$$E^{\pm} \to \sqrt{\left(\frac{\hbar}{4\epsilon_0}\right)\left(\frac{k_0}{\eta^2 a}\right)}E^{\pm}, \quad N \to \frac{N}{\mathcal{N}_0}, \quad t \to \frac{t}{L\eta/c}, \quad z \to \frac{z}{L},$$

which gives

$$\frac{\partial E^{\pm}}{\partial t} \pm \frac{\partial E^{\pm}}{\partial z} = k\left[-i\alpha N + (N-1)\left(1 + G_d\frac{\partial^2}{\partial z^2}\right) - \gamma_{int}\right]E^{\pm}, \quad (14)$$

$$\frac{\partial N}{\partial t} = j - \gamma_n N - (N-1)(|E^+|^2 + |E^-|^2) + d\frac{\partial^2 N(z,t)}{\partial z^2}, \quad (15)$$

where $k = a\mathcal{N}_0 L/2$, $\gamma_{int} = 2\alpha_i/a\mathcal{N}_0$, $j = (\mathcal{J}/\mathcal{N}_0)(L\eta/c)$, $\gamma_n = \gamma_\parallel(L\eta/c)$, and $d = (D/L^2)(L\eta/c)$. Equations (14) and (15) are supplemented with the boundary conditions

$$E^+(0,t) = \sqrt{R_1}E^-(0,t), \quad (16)$$

$$E^-(L,t) = \sqrt{R_2}E^+(L,t), \quad (17)$$

where R_1 and R_2 are the laser facet reflectivities.

III. MONOCHROMATIC SOLUTIONS

Monochromatic solutions of the form

$$\mathcal{E}(z,t) = E^+e^{i(kz-\omega t)} + E^-e^{-i(kz+\omega t)} + \text{c.c.}, \quad (18)$$

$$N(z,t) = N, \quad (19)$$

where E^+, E^-, and N are constant in time, can be identified with the longitudinal modes of the active cavity. The boundary conditions imply $\sqrt{R_1R_2}e^{2ikL} = 1$. Writing $k = k_r + ik_i$ gives

$$\sqrt{R_1R_2}e^{-2k_iL} = 1, \quad (20)$$

$$k_rL = m\pi, \quad m = 1,2,3,\ldots. \quad (21)$$

The real part of k yields the longitudinal modes k_r, while the imaginary part accounts for the loss due to the output mirrors, $k_i = \ln(R_1R_2)/(4L)$.

In the following the reference frequency ω_0 is associated with a particular longitudinal mode, the one that is closer to the maximum of the gain peak. This mode has the wave vector $k = n\pi/L + ik_i = k_0 + ik_i$ (where $k_0 = n\pi/L = \eta\omega_0/c$). With respect to this reference mode, the frequency and wave vector of the mth mode are

$$\omega_m = \omega_0 + \Delta\omega_m, \quad (22)$$

$$k_m = m\pi/L + ik_i = k_0 + ik_i + \Delta k_m, \quad (23)$$

with $\Delta k_m = (m-n)\pi/L$. Substituting in Eq. (18) we see that the forward and backward fields in terms of the dimensionless variables z and t are

$$E^{\pm}(z,t) = E^{\pm}e^{\pm i\Delta k_m Lz}e^{\mp k_iLz}e^{-i(L\eta/c)\Delta\omega_m t}, \quad (24)$$

and substituting in Eqs. (14) and (15) we obtain

$$-i\frac{L\eta}{c}\Delta\omega_m + i\Delta k_mL - k_iL = k\{-i\alpha N + (N-1)[1 + G_d(i\Delta k_mL - k_iL)^2] - \gamma_{int}\}, \quad (25)$$

$$0 = j - \gamma_n N - (N-1)(|E^+e^{-k_iLz}|^2 + |E^-e^{k_iLz}|^2). \quad (26)$$

In the equation for the carrier density the diffusion term vanishes because we are searching for solutions such that the carrier density is constant in space and time $[N(z,t)=N]$, but the equation cannot be satisfied because of the z dependence of the stimulated recombination term. However, for typical semiconductor laser parameters the mirror losses are small and $k_iL \ll 1$ [for $R_1 = R_2 = 0.95$, $k_iL = \ln(R_1R_2)/4 = -0.025$]. In this case we will search for *approximated* solutions neglecting the imaginary part of the wave vector in the carrier equation. The steady-state carrier density, frequency, and power associated with the mth longitudinal mode give

$$N_m = 1 + \frac{\gamma_{int} - k_iL/k}{1 + G_d[(k_iL)^2 - (\Delta k_mL)^2]}, \quad (27)$$

TABLE I. Laser parameters.

Value	Parameter	Description
275 μm	L	Cavity length
0.95	R_1, R_2	Output facet reflectivities
3.6	η	Background refractive index
4	α	Linewidth enhancement factor
6.4×10^{-22} m^2	a	Differential gain
10^{24} m^{-3}	$\mathcal{N}_0$	Transparency carrier density
2.53 cm^{-1}	α_i	Internal losses
0.67 ns	$\tau_n=1/\gamma_\parallel$	Carrier lifetime
65 THz	$\Delta\nu_g$	Gain bandwidth

$$\Delta\omega_m = \frac{c}{\eta L}\Delta k_m L + \frac{c}{\eta L}k[\alpha N_m + 2(N_m-1)G_d(\Delta k_m L)(k_i L)], \tag{28}$$

$$|E^+|^2 + |E^-|^2 = \frac{j-\gamma_n N_m}{N_m - 1}. \tag{29}$$

In the next section we will show that these analytic estimations are in good agreement with the results of the simulations for parameters corresponding to single-mode operation.

IV. NUMERICAL RESULTS

We simulated the model equations (14)–(17) with the dimensionless parameters $k=a\mathcal{N}_0L/2=0.088$, $\gamma_{int}=2\alpha_i/a\mathcal{N}_0=0.79$, $\gamma_n=\gamma_\parallel(L\eta/c)=0.0049$, and $G_d=7\times10^{-6}$, which correspond to the typical laser parameters indicated in Table I. The integration steps are 0.917 μm and 0.011 ps (which in dimensionless units are $\Delta z=\Delta t=1/300$). The initial conditions are with the optical fields at the noise level and the carrier density at approximately the transparency value. The results are presented for $D=0$, because, as discussed in the Introduction and shown in the previous section, the fast-grating terms that would be washed out by carrier diffusion have been neglected. We also checked that the results are unaffected when carrier diffusion is included (as shown in Fig. 6 below), due to the fact that a realistic level of carrier diffusion is too small to wash out the slow-grating component.

Near threshold the laser operates in a single longitudinal mode, whose frequency and output power agree well with the analytic estimations of the previous section, as shown in Fig. 1. The laser operates on the longitudinal mode with maximum gain (the one closest to the gain peak). As the injection current increases the dynamics remains single mode, but there is a frequency shift toward the negative frequency side (Fig. 2), which is in very good agreement with the experimental observations (see, e.g., Fig. 2 of [2]). It is well known that this frequency shift is due to the phase-amplitude coupling: indeed, if the sign of α is changed, a shift toward the positive-frequency side occurs in our simulations. At larger injection levels the dynamics becomes multimode, and several peaks appear in the optical spectrum, the dominant mode having further shifted to the red, as is also shown by the experiments [2].

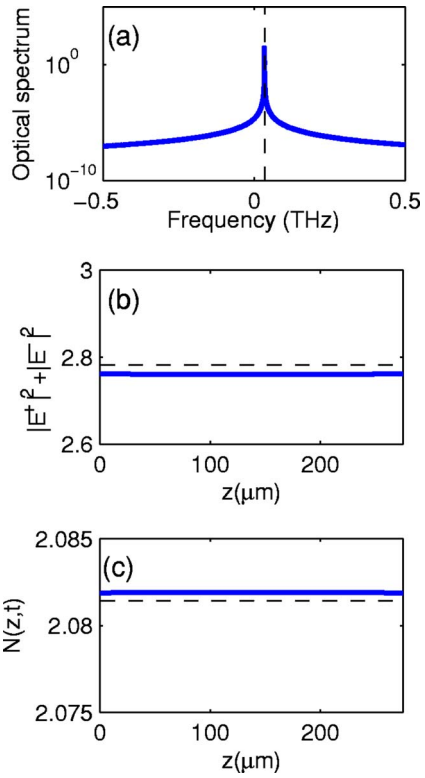

FIG. 1. (Color online) Single-longitudinal-mode behavior near threshold: optical spectrum (a), slowly varying optical intensity (b), and carrier density (c) in the laser cavity. The dashed lines indicate the values predicted by the approximated analytical expressions (27)–(29). $j=0.0105$; other parameters are indicated in Table I.

In the multimode regime the output power exhibits fast oscillations due to mode beating. To investigate the underlying longitudinal-mode dynamics we applied a standard filtering technique in the frequency domain, and obtained the modal optical fields by convolution of $E^+(z=0,\omega)+E^-(z=0,\omega)$ with a filter centered at the different modal frequencies. By inverse transforming we calculated the time-dependent modal intensities $I_m(t)=|E_m(t)|^2$ and the incoherent intensity sum

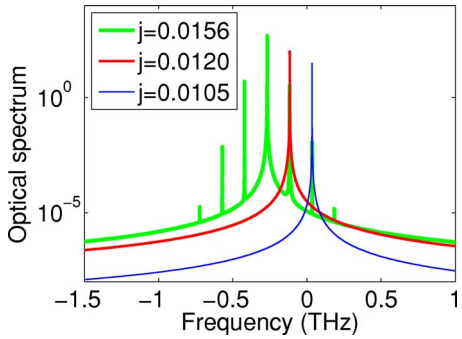

FIG. 2. (Color online) Optical spectrum for $j=0.0105$ (thin line, blue online), $j=0.012$ (red online), and $j=0.0156$ (thick line, green online).

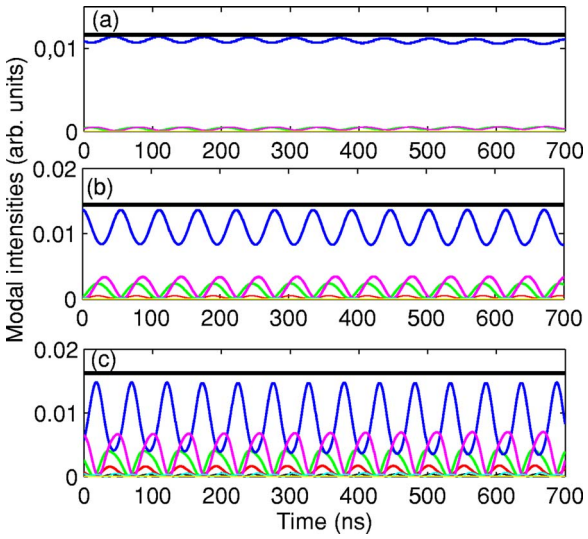

FIG. 3. (Color online) Modal intensities (thin lines) and incoherent sum (thick black line) for $j=0.0165$ (a), 0.018 (b), and 0.019 (c).

$$I(t) = \sum_m |E_m(t)|^2. \tag{30}$$

We found that the modal intensities exhibit anticorrelated oscillations that result in a complete compensation of the incoherent sum (Fig. 3). There is a deterministic constant phase relationship between the oscillations of the longitudinal modes, as can be observed in Figs. 3(a)–3(c), which prevails if the simulations are done with different initial conditions. Near the onset of multimode operation, however, we see very long transients before the modal oscillations reach their deterministic phase and amplitude relation. As the injection current increases those transients become shorter, the amplitude of the oscillations becomes larger, the dynamics becomes faster, and the number of active longitudinal modes increases; always, compensation of the incoherent sum is maintained (see Figs. 3–6). These results are in good qualitative agreement with the observations of [1].

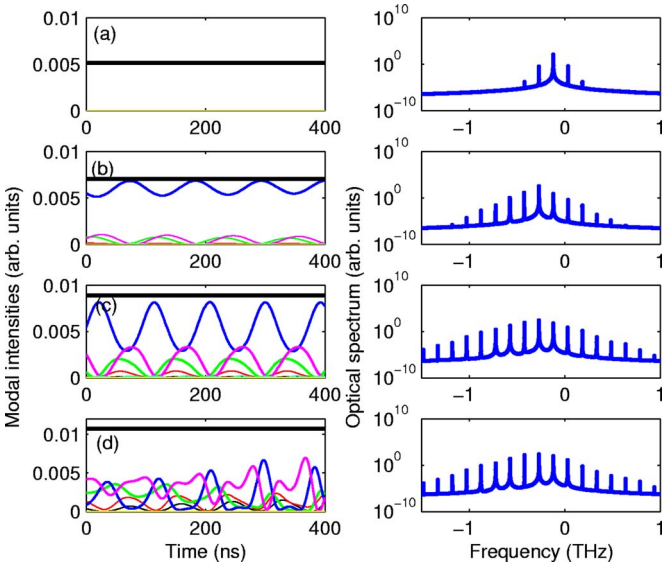

FIG. 5. (Color online) Modal oscillations (left) and optical spectrum (right) for larger gain bandwidth ($G_d=4\times10^{-6}$). j= (a) 0.013, (b) 0.014, (c) 0.015, and (d) 0.016. Note that the modal phase and amplitude relations are as in Fig. 2.

For even larger injection, the modal oscillations become chaotic and there is an alternation of the mode that dominates the emission, as shown in Fig. 4. The instability scenario for increasing injection current shown in Figs. 3 and 4 occurs also for other parameter values, as shown in Fig. 5, the regions of single and multimode operation for a given value of the injection current j varying with the gain bandwidth [10,11], and is robust to the inclusion of carrier diffusion (as shown in Fig. 6).

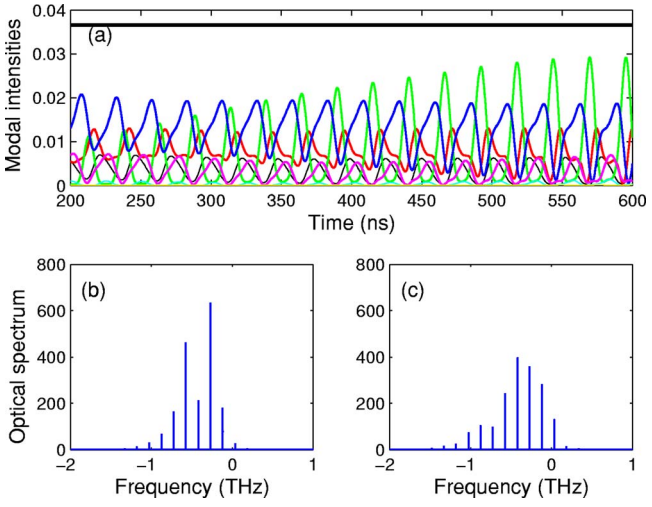

FIG. 4. (Color online) (a) Modal oscillations (thin lines) and incoherent sum (thick black line) for $j=0.03$. (b),(c) Optical spectra done in different time intervals reveal the alternation of the dominant longitudinal mode.

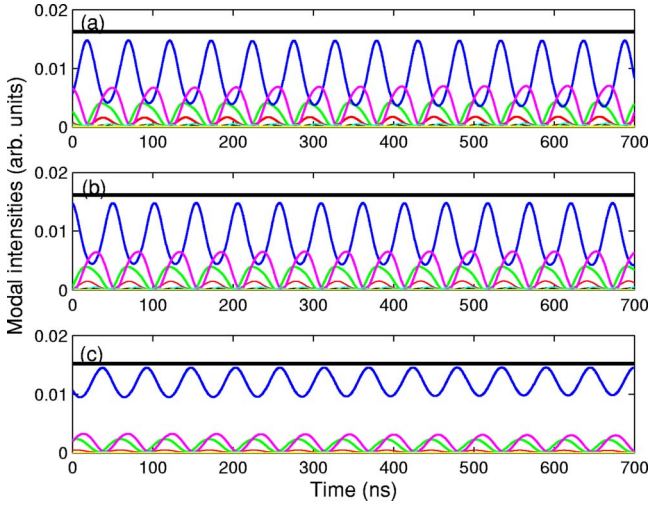

FIG. 6. (Color online) Influence of carrier diffusion. $G_d=7\times10^{-6}$, $j=0.019$. d= (a) 0, (b) 10^{-6} ($D=0.023$ m^2 s^{-1}), and (c) 10^{-5} ($D=0.229$ m^2 s^{-1}).

V. CONCLUSIONS

In conclusion, we have investigated the emission in a multi-longitudinal-mode semiconductor laser by using traveling-wave deterministic rate equations. In spite of the approximations of the model, which takes into account a simple parabolic frequency-dependent gain, the model reproduces qualitatively well the observed multi-longitudinal-mode behavior in semiconductor lasers, such as antiphase modal oscillations which leave the sum of total modal intensities nearly constant, near-threshold mode switching, and hopping dynamics. While more sophisticated models, like the ones presented in Ref. [2], have the advantage of achieving a more quantitative (and not only qualitative) agreement with the experimental observations, our model has the advantage that it does not obscure the roots of such multimode behavior, which can be traced down to the spatial hole-burning effect on the slowly varying envelope of the carrier density, due to the superposition of various longitudinal modes. On the other hand, while spontaneous emission and carrier noise play important roles in the dynamics of semiconductor lasers, in this study we have not taken into account any source of stochastic behavior because the aim of our work was the study of the deterministic modal oscillations induced by spatial effects. The study of the interplay of stochastic and deterministic behavior is in progress and will be reported elsewhere.

[1] A. M. Yacomotti, L. Furfaro, X. Hachair, F. Pedaci, M. Giudici, J. Tredicce, J. Javaloyes, S. Balle, E. A. Viktorov, and P. Mandel, Phys. Rev. A **69**, 053816 (2004).
[2] L. Furfaro, F. Pedaci, M. Giudici, X. Hachair, J. Tredicce, and S. Balle, IEEE J. Quantum Electron. **40**, 1365 (2004).
[3] M. Ahmed and M. Yamada, IEEE J. Quantum Electron. **38**, 682 (2002).
[4] M. Ahmed, Physica D **176**, 212 (2003).
[5] L. Furfaro, F. Pedaci, J. Javaloyes, X. Hachair, M. Giudici, S. Balle, and J. Tredicce, IEEE J. Quantum Electron. **41**, 609 (2005).
[6] M. Homar, J. V. Moloney, and M. San Miguel, IEEE J. Quantum Electron. **32**, 553 (1996).
[7] M. Homar, S. Balle, and M. San Miguel, Opt. Commun. **131**, 380 (1996).
[8] J. K. White *et al.*, IEEE J. Quantum Electron. **34**, 1469 (1998).
[9] G. Huyet, J. K. White, A. J. Kent, S. P. Hegarty, J. V. Moloney, and J. G. McInerney, Phys. Rev. A **60**, 1534 (1999).
[10] C. Serrat, S. Prins, and R. Vilaseca, Phys. Rev. A **68**, 053804 (2003).
[11] C. Serrat, B. Le Ny, and R. Vilaseca, J. Opt. B: Quantum Semiclassical Opt. **6**, 472 (2004).
[12] J. K. White and J. V. Moloney, Phys. Rev. A **59**, 2422 (1999).
[13] C. Masoller, M. S. Torre, and P. Mandel, Phys. Rev. A **71**, 013818 (2005).
[14] C. Etrich, P. Mandel, N. B. Abraham, and H. Zeghlache, IEEE J. Quantum Electron. **28**, 811 (1992).